Rock and Soil Mechanics

Volume 41 | Issue 8 Article 3

1-22-2021

Study on simulation method of mode I fracture toughness and its meso-influencing factors

Shun-chuan WU
Faculty of Land Resource Engineering, Kunming University of Science and Technology, Kunming, Yunnan 650093, China

Wei SUN
Key Laboratory of Ministry of Education for Efficient Mining and Safety of Metal Mine, University of Science and Technology Beijing, Beijing 100083, China

Yang LIU
Key Laboratory of Ministry of Education for Efficient Mining and Safety of Metal Mine, University of Science and Technology Beijing, Beijing 100083, China

Zi-qiao CHENG
PowerChina Roadbridge Group Co., Ltd., Beijing 100044, China

See next page for additional authors

Custom Citation

WU Shun-chuan, SUN Wei, LIU Yang, CHENG Zi-qiao, XU Xue-liang, . Study on simulation method of mode I fracture toughness and its meso-influencing factors[J]. Rock and Soil Mechanics, 2020, 41(8): 2536-2546.

Study on simulation method of mode I fracture toughness and its meso-influencing factors

Authors

Shun-chuan WU, Wei SUN, Yang LIU, Zi-qiao CHENG, and Xue-liang XU

Rock and Soil Mechanics 2020 41(8): 2536−2546 ISSN 1000−7598
https: //doi.org/10.16285/j.rsm.2019.7064 rocksoilmech.researchcommons.org/journal

Study on simulation method of mode I fracture toughness and its meso-influencing factors

WU Shun-chuan[1, 2], SUN Wei[1], LIU Yang[1], CHENG Zi-qiao[3], XU Xue-liang[4]

1. Key Laboratory of Ministry of Education for Efficient Mining and Safety of Metal Mine, University of Science and Technology Beijing, Beijing 100083, China
2. Faculty of Land Resource Engineering, Kunming University of Science and Technology, Kunming, Yunnan 650093, China
3. PowerChina Roadbridge Group Co., Ltd., Beijing 100044, China
4. Railway Engineering Research Institute, China Academy of Railway Sciences, Beijing 100081, China

Abstract: The discrete element numerical method has been usually used for some parameter sensitivity analysis of geo-materials in the compression test and the Brazilian splitting test. However, there have been limited studies systematically focusing on mesoscopic influencing factors and 3D fracture process in mode I fracture toughness tests. The 2D discrete element methods cannot reflect the real mechanical behavior of a 3D model. Therefore, a three-dimensional flat joint model (FJM3D) is used in this paper to investigate the effects of microstructure parameters and bond mesoscopic parameters on mode I fracture toughness tests with different notch shapes. The microstructure parameters include the square root of average particle radius ($\sqrt{R}$), model resolution (Ψ), and maximum/minimum particle diameter ($d_{\max}/d_{\min}$). Bond meso-parameters include average coordination number (CN), slit element fraction (φ_s), bond tensile strength (σ_b), bond cohesion (c_b), friction coefficient (μ) and friction angle (φ). Results of parameter sensitivity analysis show that the mode I fracture toughness (K_{Ic}) is positively correlated with $\sqrt{R}$, CN, and σ_b, and negatively correlated with $d_{\max}/d_{\min}$ and φ_s. There are no obvious linear relationships between K_{Ic} and Ψ, c_b, μ, φ. In addition, suitable ranges of Ψ and $d_{\max}/d_{\min}$ are recommended to obtain an appropriate mode I fracture toughness with a low level of variation. Based on the results of parameter sensitivity analysis, the mechanical behaviors of the Kowloon granite with notched semi-circular bend (SCB) and cracked chevron notched semi-circular bend (CCNSCB) specimens are calibrated. The failure process of mode I fracture toughness tests with different notch shapes indicates that the pre-peak and post-peak behaviors of the SCB test is more consistent with the laboratory test.

Keywords: mode I fracture toughness; flat-joint model; sensitivity analysis; SCB; CCNSCB

1 Introduction

Rock fracture toughness is an important parameter to describe rock resistance to crack initiation and propagation, which can be used to identify and predict the immediate damage of rock mass structures, and provide guidance for improving the stability and safety of rock mass structures. In addition, it can guide the development of new technologies for mineral resources, such as mechanized mining, blasting, hydraulic fracturing, etc.[1–2].

Due to high compressive strength and low tensile strength of rocks, mode I fracture (open or tensile type) is regarded as the most basic and important type in rock fracture mechanics. The semi-circular bend (SCB) method is recommended by International Society for Rock Mechanics (ISRM) for mode I fracture toughness, and it has received much attention in the field of rock fracture[3–4]. For the laboratory measurements, there are currently four methods to measure the mode I fracture toughness, including chevron bend (CB) test, short rod (SR) test, cracked chevron notched Brazilian disc (CCNBD) test , and semi-circular bend (SCB) test. Compared with CB, SR and CCNBD methods, SCB has several advantages: (1). the specimen preparation is simple and the specimen size is small; (2). the loading equipment is relatively simple, and the three-point bending load is applied by commonly used compression equipments; (3). the fracture toughness can be calculated with only the maximum load. The cracked chevron notched semi-circular bend (CCNSCB) specimen can be regarded as half of the CCNBD specimen in app- earance, which essentially eliminates the assumption of symmetrical crack propagation in the CCNBD test. Therefore, it is a improvement of the CCNBD method. In recent years, the CCNSCB method has attracted a lot of attention due to its advantages, but its progressive fracture process has not yet been effectively evaluated. Some scholars[6–8] used the SCB and CCNSCB methods to measure the mode I fracture toughness (K_{Ic}) of the same kind of rock, and they found that the fracture toughness of CCNSCB specimens was generally higher than that of SCB specimens. However, the essential reasons for the above results have not yet been revealed. In numerical sim-

Received: 9 December 2019 Revised: 20 May 2020
This work was supported by the National Natural Science Foundation of China(51774020, 51934003), the National Key Research and Development Program of China (2017YFC0805300) and the Science and Technology Project of Power China Road Bridge Group Co., Ltd. (LQKY2017-03).
First author: WU Shun-chuan, male, born in 1969, PhD, Professor, PhD supervisor, focusing on geotechnical disaster prevention and control. E-mail: wushunchuan@ustb.edu.cn
Corresponding author: Sun Wei, male, born in 1987, PhD candidate, focusing on rock fracture mechanics and numerical simulation. E-mail: sunweiustb@outlook.com

ulations, Potyondy et al.[9] used the bonded-particle model (including contact bonds and parallel bonds) to obtain mode I fracture toughness and found that particle size was not a free parameter. The FJM3D (three-dimensional flat joint model) was applied by Xu[2] for CCNSCB and fracture toughness was found to be linearly positively correlated with bond tensile strength, and the square root of the particle diameter, and negatively correlated with the square root of the maximum and minimum particle ratio. Overall, the response of the meso-parameters of different fracture toughness test methods or contact models can be quite different.

At present, investigation of mode I fracture toughness tests by discrete element is mainly based on the standard BPM model, which is mostly 2D model. However, the 2D model cannot truly reflect the fracture process of 3D specimens. Most sensitivity analysis of parameters is for the compression test and the Brazilian splitting test and there are limited studies for SCB and CCNSCB tests. In the mode I fracture toughness test, the straight-through notch and the cracked chevron notch are the most used shapes, but the role played by different notch shapes has not been fully understood. Based on this, it is necessary to use the widely used FJM3D model for numerical evaluation of the SCB and CCNSCB methods. First, a set of modelling method for fracture toughness that meets the smoothness requirements is developed, and the influence of mesostructure and meso-parameters of the FJM3D model on mode I fracture toughness is systematically studied. Based on the results of para- meter sensitivity analysis, the mechanical behaviors of the Kowloon granite are calibrated, providing suggestions for calibrations of meso-parameters in mode I fracture toughness tests. Finally, the mode I fracture process of SCB and CCNSCB specimens with different notch shapes is analyzed from a mesoscopic perspective.

2 Flat-joint mode I fracture toughness model and introduction of SCB and CCNSCB methods

2.1 Flat joint model

The particle flow code (PFC) is widely used to simulate rock mechanical behavior, especially fracture and nonlinear behavior. The calculation in PFC is performed by alternately applying Newton's second law between particles and the force-displacement law between contacts. Compared with the continuous method that indirectly characterizes fractures, PFC can directly characterize the fracture through structural unit or contact fracture without special fracture criteria[9−10]. With its unique advantages in the study of rock or rock-like fracture mechanism, the standard BPM is widely used in many fields, such as rock engineering, slope engineering, mining engineering, etc.

The FJM model is superior to the standard BPM model in reproducing the fracture mode and macro-mechanical behavior of brittle rocks[2, 11−13]. The following is a detailed introduction of the FJM3D model from the four main aspects of solving the standard BPM defects: (1). A new bond meso-parameter installation spacing ratio is introduced to increase the self-locking effect between particles. (2). The contact mechanics behavior of FJM3D is described by equal volume elements between abstract surfaces. Each element can be bonded or non-bonded with friction, so the contact state of flat joints can be deformed, damaged or partially damaged.(3). Flat joint contacts include bonded elements (type B) and non-bonded elements (types G and S). The model is randomly assigned to the intermediate contact surface between particles according to the proportions of the three types of elements. The non-bonded elements are used as pre-cracks in the model to simulate natural defects such as pores or cleavage in the tight rock. (4). The stress-related shear strength is introduced. The shear strength of the bonded element follows the Coulomb criterion with tension cut-off, and the non-bonded element follows the Coulomb slip criterion, as shown in Figs.1(b) and 1(c). Among them, points 1–3 are to modify the contact microstructure parameters, and the point 4 is to modify the constitutive relationship. The FJM3D model has been improved from the above aspects and the three major characteristics of brittle rocks including high tension compression ratio, large friction angle and nonlinear envelope can be well reproduced. More detailed descriptions of the FJM3D mechanism can be found in the literatures[2, 13], which will not be repeated here.

2.2 Numerical model of model I fracture toughness

In traditional modeling methods of SCB and CCNSCB tests, a semicircle is usually cut off from a cuboid[14−16] and the notch is generated by deleting particles. The wide wall or traditional cylindrical support is used as the upper support[17]. There are some problems existing in these methods such as uneven circumference and notch, insufficient contact between supports and particles, which makes it easy to fail when loading the model. Although a smaller particle diameter can relatively improve the smoothness of the disc surface, it increases the calculation amount of the model. A set of I-type fracture toughness test modeling method (see Fig.2) is developed in this article, and the steps are as follows:

(1) The multiple narrow bars are regarded as a cylinder when generating a disc, and a dividing wall is inserted in the middle to divide the disc into half circles. The smoothness of the circumference, front and rear surfaces and bottom surface of the semicircle model is ensured, and the smoothness of the circumference and the lower support is controlled by the circumference resolution.

(2) The narrow wall acts as the top support, and the cylinder generates the bottom support to ensure that the support is in full contact with the particles.

(3) The straight-through notch and the cracked chevron notch are generated by a cuboid and a double semicircle of discrete fracture network (DFN), which avoids the serrated grooving produced by the traditional method and meets the smoothness requirements for notches.

The circumferences of numerical specimens of SCB and CCNSCB composed of 39 narrow bars gen-

erated by the above method and the notches generated by DFN are very smooth, which meets the requirements of full load contact and smoothness.

2.3 SCB test and CCNSCB test method

Figure 3(a) shows a schematic diagram of the geometric dimensions of the SCB specimen, and the corresponding symbol annotations and adopted dimensions are listed in Table 1. The numerical specimen is composed of 4472 particles and is kept under quasi-static loading at a rate of 0.004 m/s until failure. Using the maximum load P_{max} and geometric parameters obtained above, the calculation formula of K_{Ic} is as follows[3]:

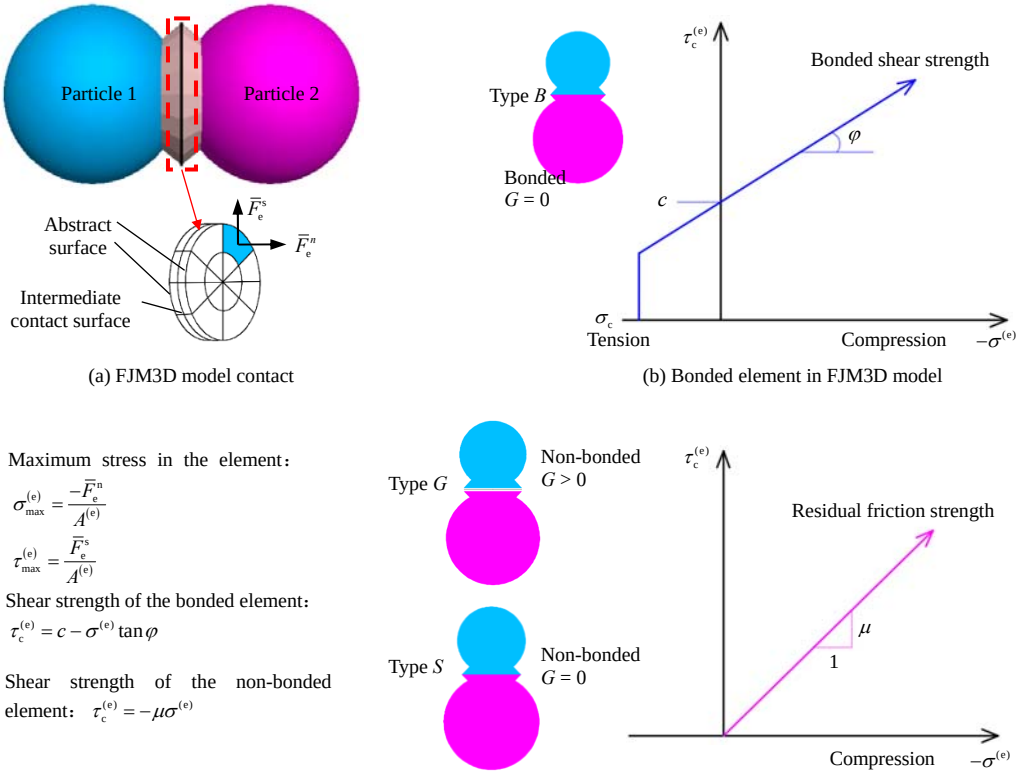

(a) FJM3D model contact

(b) Bonded element in FJM3D model

(c) Non-bonded element in FJM3D model

Fig. 1 Meso-structure and force-displacement of FJM3D

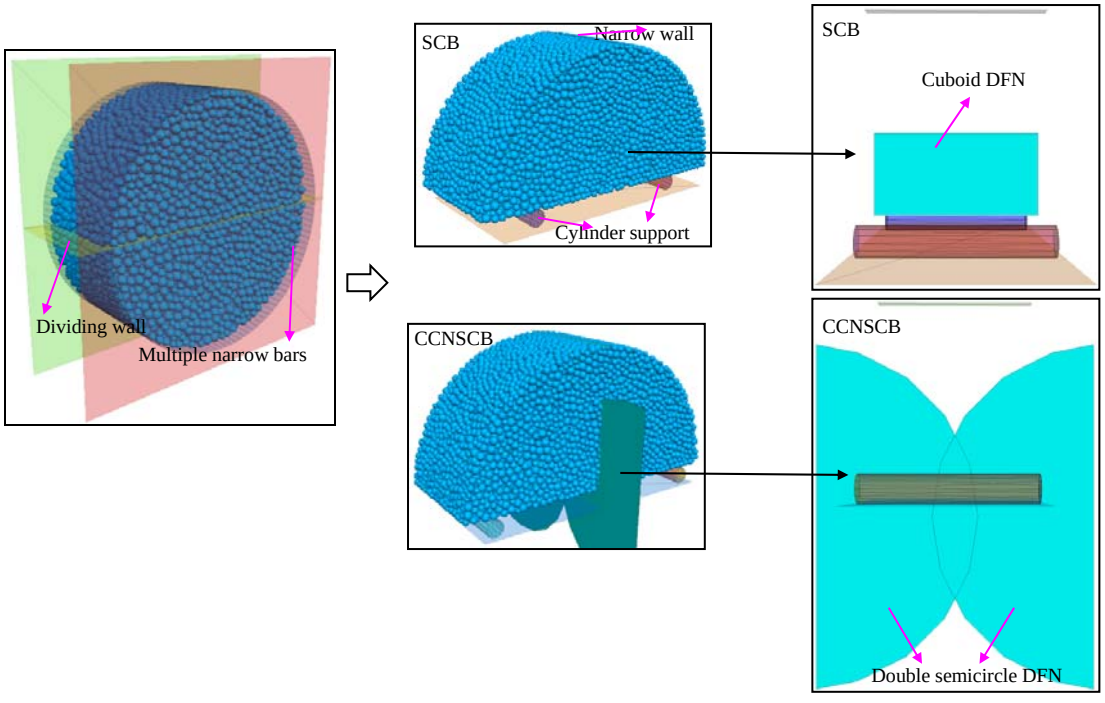

(a) Approximately smooth semicircular disk (b) Three-point bending support (c) Smooth notch generated by DFN

Fig. 2 Generation method of FJM3D model for mode I fracture toughness

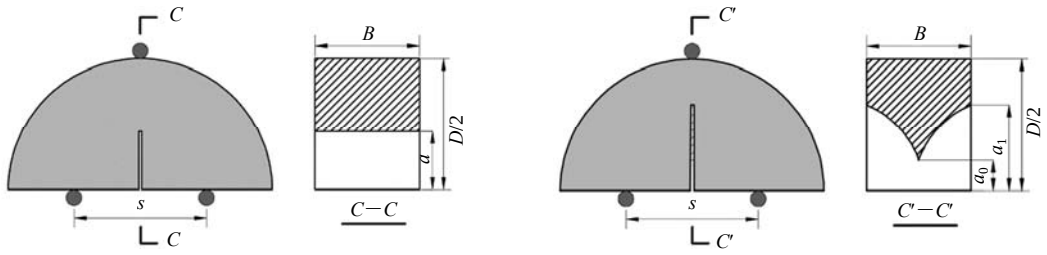

(a) SCB specimen (b) CCNSCB specimen

Fig. 3 Geometrical dimensions of mode I fracture toughness specimen

$$K_{\mathrm{Ic}} = Y' \frac{P_{\max}\sqrt{\pi a}}{2RB} \tag{1}$$

$$Y' = -1.297 + 9.516(s/2R) - [0.47 + 16.457 \cdot (s/2R)]\beta + [1.071 + 34.401(s/2R)]\beta^2 \tag{2}$$

where $\beta = a / R$; Y' is the critical stress intensity factor, with a value of 2.905.

Figure 3(b) shows a schematic diagram of the geometric dimensions of the CCNSCB specimen, and the corresponding symbol annotations and adopted dimensions are listed in Table 2. The particle composition and loading rate of the numerical specimen are consistent with the SCB test. The maximum load $P_{\max}$ and geometric parameters are used in the calculation of K_{Ic} [6]:

$$K_{\mathrm{Ic}} = Y' \frac{P_{\max}}{B\sqrt{R}} \tag{3}$$

Table 1 Recommended geometrical dimensions of SCB specimen

Parameter	Value or range recommended by ISRM	Parameter values in numerical test model / mm
Diameter D	Larger than 10 times of particles diameter or 76 mm	75.0
Thickness B	Larger than 0.4D or 30 mm	30.0
Straight notch length a	$0.4 \leqslant 2a/D \leqslant 0.6$	15.0
Support spacing s	$0.5 \leqslant s/D \leqslant 0.8$	37.5

Table 2 Recommended geometrical dimensions of CCNSCB specimen

Parameter	Recommended value or range	Parameter values in numerical test model / mm
Diameter D	75 mm	75.00
Thickness B	$0.44 \leqslant B/R \leqslant 1.04$	30.00
Minimum chevron notch length a_0	a_0/R =0.263 7	9.89
Maximum chevron notch length a_1	$0.4 \leqslant a_1/R \leqslant 0.8$	24.38
Support spacing s	—	37.50

3 Meso-influencing factors for mode I fracture toughness

The meso-influencing factors used for sensitivity analysis are divided into two categories: microstructure parameters and bond meso-parameters. The microstructure parameters include the square root of average particle radius $\sqrt{R}$, model resolution Ψ, and maximum/minimum particle diameter $d_{\max} / d_{\min}$. Bond meso-parameters include average coordination number CN, S-type element fraction φ_{s}, bond tensile strength σ_{b}, bond cohesion c_{b}, friction coefficient μ, and friction angle φ. Five to six groups of values are set for each parameter. In each group, five random seeds are used to generate different arrangements. The control variable method using single factor is adopted: when the influence of a certain factor is considered, other parameters remain unchanged.

3.1 Effects of meso-structure parameters on K_{Ic}

The values of $\sqrt{R}$ are set to be 0.80, 0.977, 1.127, 1.238 and 1.377 mm, respectively; the values of Ψ are set to be 5, 8, 11.8, 14, 16.6 and 20, respectively; and the values of $d_{\max} / d_{\min}$ are set to be 1:1, 1.3:1, 1.66:1, 2:1, 2.25:1 and 2.5:1. The relationship between K_{Ic} and meso-influencing factors is displayed in Fig.4. The average value and standard deviation of K_{Ic} obtained from the SCB and CCNSCB tests increase linearly with $\sqrt{R}$. The increasing rate (about 0.51 to 0.55) is basically the same, and the effect of $\sqrt{R}$ on both K_{Ic} values is also the same. In addition, with the same $\sqrt{R}$, the average value of K_{Ic} obtained by CCNSCB is greater than that of SCB, which is about 22% higher than that of SCB. There is no obvious linear correlation between the average value of K_{Ic} and Ψ, and the standard deviation is negatively correlated with Ψ. Moreover, the standard deviation obtained by the model with Ψ greater than 11.8 is smaller. It is recommended that the resolution of the SCB and CCNSCB numerical specimens should be kept above 11.8. The average value of K_{Ic} and standard deviation decrease linearly with $d_{\max} / d_{\min}$, and the decreasing rate of CCNSCB is greater than that of SCB. With the same $d_{\max} / d_{\min}$, the average value of K_{Ic} obtained by CCNSCB is greater than that of SCB, which is about 21% higher than that of SCB. There is a small fluctuation when $d_{\max} / d_{\min}$ is smaller than 2. Therefore, it is better to keep the value of $d_{\max} / d_{\min}$ between 1 and 2 in the numerical simulation of SCB and CCNSCB.

3.2 Effects of bond meso-parameters on K_{Ic}

3.2.1 Effect of average coordination number CN on K_{Ic}

The average coordination numbers CN are set to be 7.6, 8.2, 9, 9.7, 10.5 and 11.5, respectively. A positive correlation between K_{Ic} and CN is observed

in Fig.5. A larger CN indicates that there are more flat joint contacts around the particles, which means that the self-locking effect of the particles is enhanced, and a greater stress is required to destroy particle contact. In addition, K_{Ic} obtained in the CCNSCB test is greater than that of the SCB test.

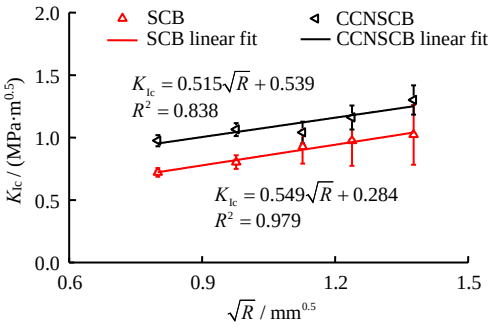

(a) Square root of average particle radius

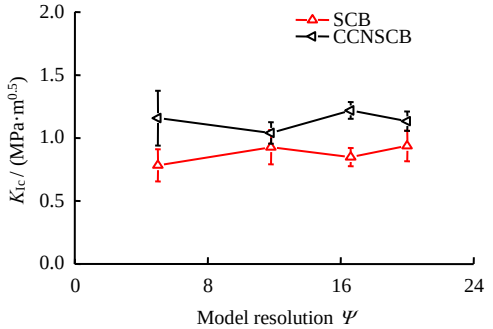

(b) Model resolution Ψ

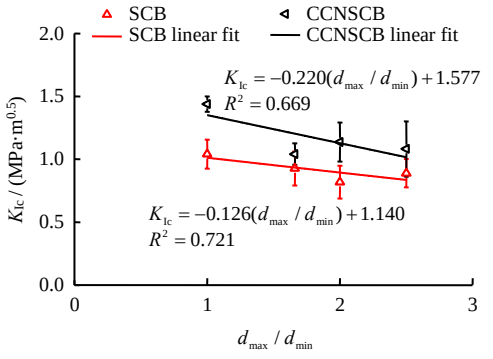

(c) Maximum/minimum particle diameter d_{max} / d_{min}

Fig. 4 Effects of meso-structure parameters on mode I fracture toughness K_{Ic}

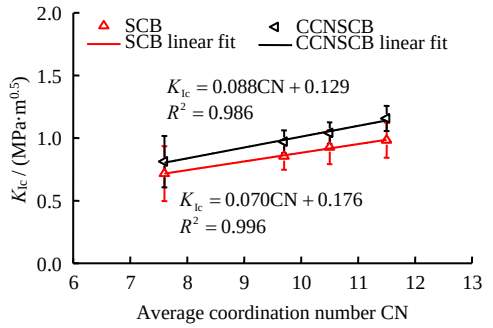

Fig. 5 Effect of average coordination number CN on mode I fracture toughness K_{Ic}

3.2.2 Effect of S-type element fraction φ_s on K_{Ic}

The S-type element fractions φ_s are set to be 0.1, 0.2, 0.3, 0.4 and 0.5. Figure 6 shows that K_{Ic} obtained from both the SCB and CCNSCB tests decreases with increasing φ_s. The increasing φ_s indicates an increase of the crack density of the model, which damages the integrity of the bond chain between the particles. Then the fracture stress of the specimen decreases accordingly. For a low crack density ($\varphi_s \leqslant 0.3$), the decreasing rate of SCB is larger than CCNSCB; for a high crack density ($\varphi_s \geqslant 0.3$), the decreasing rate of SCB is smaller than CCNSCB. The CCNSCB tests are more sensitive to φ_s in cases of a high crack density.

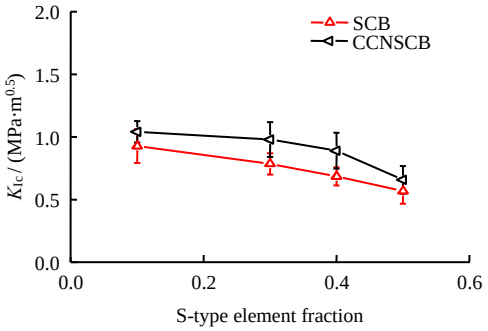

Fig. 6 Effect of S-type element fraction φ_s on mode I fracture toughness K_{Ic}

3.2.3 Meso-strength parameters

To investigate the influence of the bond meso-strength parameters on K_{Ic}, six different values are chosen for bond cohesion c_b, bond tensile strength σ_b, friction coefficient μ, and friction angle φ. The relationships between K_{Ic} and c_b, σ_b, μ and φ are displayed in Fig.7.

K_{Ic} is only linearly correlated with σ_b. In addition, K_{Ic} obtained in the SCB test is smaller than in the CCNSCB test, and the rate of increase is smaller than CCNSCB. The linear fitting equation between σ_b and K_{Ic} obtained in the SCB test is as follows:

$$K_{Ic} = 0.046\sigma_b + 0.014,\ R^2 = 0.999 \quad (5)$$

The linear fitting equation between σ_b and K_{Ic} obatined in the CCNSCB test is as follows:

$$K_{Ic} = 0.055\sigma_b - 0.046,\ R^2 = 0.996 \quad (6)$$

The correlation coefficients of the above two fitting relations are close to 1, which well confirms the conclusions derived by Potyondy et al.[9]. However, there are still some differences between these two relationships. The intercepts of the linear fitting equations of the SCB and CCNSCB tests are 0.014 MPa·m$^{0.5}$ and -0.046 MPa·m$^{0.5}$, respectively; and the non-zero intercept is caused by fracturing-induced tension failure. The other three strength parameters c_b, μ, and φ have basically no effect on K_{Ic}. μ and φ control the post-peak behavior of the load-displacement curve in the compression test and the friction angle in the model, separately. No matter how μ and φ change, K_{Ic} obtainned in the SCB and CCNSCB tests remains unchanged, and the former is smaller than the latter.

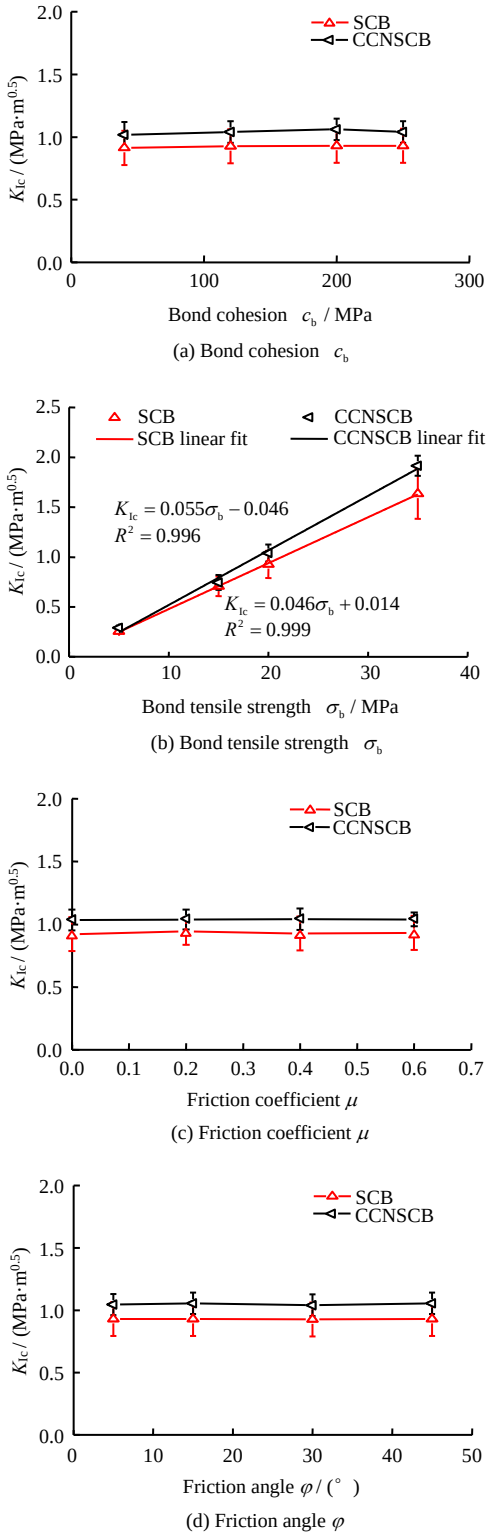

Fig. 7 Effect of bond strength on mode I fracture toughness K_{Ic}

4 Meso-analysis of mode I fracture toughness test of the Kowloon granite

4.1 Calibration of mode I fracture toughness in FJM3D model

The Kowloon granite[8] in the northwest of Hong Kong Island is investigated in this study. This rock is a medium-grained granite with an average grain diameter of 0.92 mm. It is mainly composed of 54.2% quartz, 23.2% potassium feldspar, and 13.8% plagioclase and 8.9% biotite. The radius of the SCB specimen is 42 mm, the thickness is 36 mm, the length of the prefabricated straight-through notch is 21 mm, and the distance between the double supports is 25.2 mm, which is consistent with the recommended value or range of ISRM[3]. The same radius and thickness of the CCNSCB specimen are chosen as the SCB, with the minimum length of the prefabricated chevron notch of 11.08 mm, the maximum length of 27.3 mm, and the distance between the double supports of 33.6 mm. The MTS815 servo-controlled testing system for rock mechanics equipped with a three-point bending fixture is used for fracture toughness test. The average value obtained from the six groups of SCB specimens is 1.24 MPa·m$^{0.5}$ with the standard deviation of 0.05 MPa·m$^{0.5}$; the average value obtained in the seven groups of CCNSCB specimens is 1.94 MPa·m$^{0.5}$ with the standard deviation of 0.17 MPa·m$^{0.5}$.

The size of the FJM3D model used to simulate the mode I fracture toughness of the Kowloon granite is consistent with the laboratory test, and the quasi-static loading is maintained at a rate of 0.004 m/s. The average value and standard deviation of results in the SCB numerical test in Table 4 are basically the same as the indoor tests, which has a good agreement with the mode I fracture toughness of the rock. Figure 8 shows the load–displacement curves of the SCB and CCNSCB specimens in numerical tests and indoor tests using the parameters in Table 3. Most mechanisms of the mode I fracture of the Kowloon granite (except for compaction stage), such as deformation characteristics, peak load, and post-peak behavior can be reproduced in the SCB numerical test. At present, the pore compaction process similar to that of natural specimens cannot be realized in the FJM model. The average value and standard deviation of results in the CCNSCB numerical tests in Table 4 are smaller than those of the laboratory tests. However, the deformation characteristics are consistent, and the slopes (elastic modulus) of the straight-line segments of the two curves are approximately equal. Unlike the indoor test, a local peak is observed in the peak load–displacement curve of the CCNSCB numerical test. A sharp drop for the post-peak behavior does not occur at the minimal displacement, and a drop step by step is witnessed. According to the analysis in Section 3.1, an increase of $\sqrt{R}$ and a decrease of d_{max}/d_{min} can increase K_{Ic}, and now d_{max}/d_{min} is reduced to 1.0. The black dashed line in Fig.8(b) shows the load–displacement curve after the adjustment of d_{max}/d_{min}. It can be seen that the peak value of mode I fracture obtained in the numerical model increases, which can well match the peak load of the indoor test. Meanwhile, d_{max}/d_{min} also has a certain influence on the deformation characteristics. When the mesoscopic parameters can be matched with the mode I fracture load-displacement curve of the SCB specimens, K_{Ic} obtained in CCNSCB specimens with the corresponding parameters is too small.

Table 3 Meso-parameters used to simulate Kowloon granite

Contact model	Property	Basic value
Flat joint	Minimum particle diameter d_{min} / mm	1.5
	Maximum/ minimum particle diameter d_{max}/d_{min}	1.66
	Installation spacing ratio g_{ratio}	0.4
	Number of radial elements N_r	1
	Number of elements in the circumferential direction N_a	3
	S-type element fraction φ_s	0.1
	Effective modulus of particle and bond $E_c = \bar{E}_c$ / GPa	10.5
	Normal to tangential stiffness ratio of particle and bond $k_n/k_s = \bar{k}_n/\bar{k}_s$	1.5
	Bond tensile strength and standard deviation σ_b / MPa	35±0
	Bond cohesion and standard deviation c_b / MPa	220±0
	Friction coefficient μ	0.4
	Friction angle φ / (°)	0
	Installation spacing ratio g_0	0
	Friction coefficient μ	0.5
Smooth joint	Normal strength of bonding system / MPa	0
	Tangential strength of bonding system / MPa	0
	Friction angle of bonding system / (°)	0

Table 4 Results of Kowloon granite obtained from laboratory tests[8] and FJM3D simulations

Mode I fracture toughness test	Laboratory	Simulation
SCB test P_{max} / kN	3.20±0.382(n=6)	3.26±0.085(n=4)
SCB test K_{Ic} / (MPa·m$^{0.5}$)	1.24±0.05(n=6)	1.38±0.036(n=4)
CCNSCB test P_{max} / kN	2.54±0.250(n=7)	2.13±0.055(n=4)
CCNSCB test K_{Ic} / (MPa·m$^{0.5}$)	1.94±0.17(n=7)	1.74±0.045(n=4)

Note: n represents the number of trials or the number of random seeds.

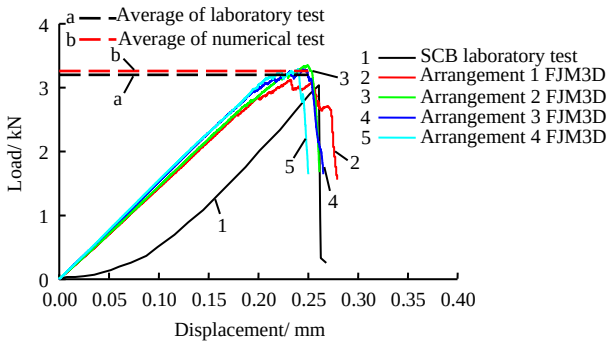

(a) SCB test

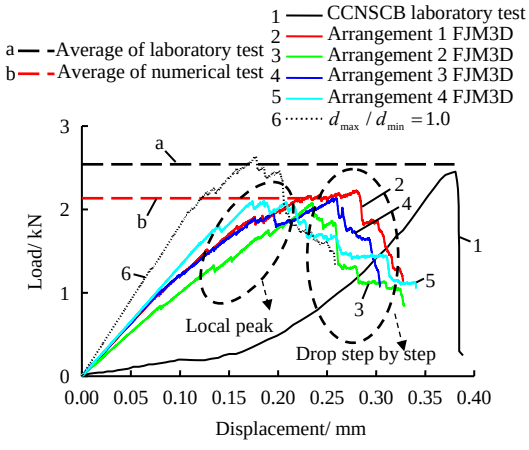

(b) CCNSCB test

Fig. 8 Stress–strain curves of mode I fracture toughness tests

4.2 Numerical test process of mode I fracture toughness in FJM3D

The five side views in Fig. 9 correspond to points *a*, *b*, *c*, *d*, and *e* of the load–displacement curve, n_T and n_S indicate the number of tension cracks and shear cracks, respectively. According to the crack growth distribution, the meso-scale numerical model I fracture toughness test of SCB is divided into three stages: the initiation of the straight-through notch tip (point *a*), the stable growth of the straight-through notch (points *a*–*c*) and the penetrating stage (points *c*–*e*). At the initiation stage of the straight-through notch tip, the initiation cracks are scattered at the tip of straight-through notch, all of which are tensile cracks. Moreover, the number of cracks is about 5% of the total number of cracks at the peak. The load at load point *a* is 2.58 kN, which is about 79% of the peak load. Then the load is applied to point *b*, and the steady propagation of cracks occurs vertically upwards. The cracks are all tension cracks, which are about 49% of the total number of cracks at the peak. The cracks are close to each other in space, which can be regarded as the formation

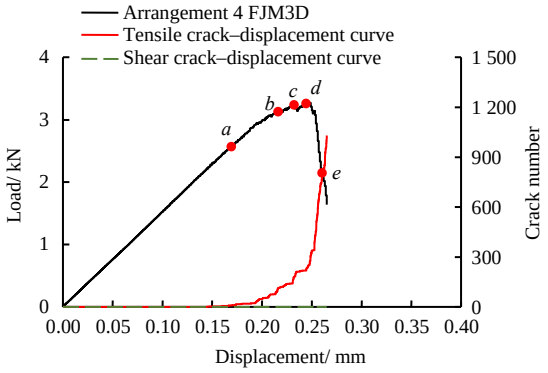

(a) Relationships between load, crack number and displacement

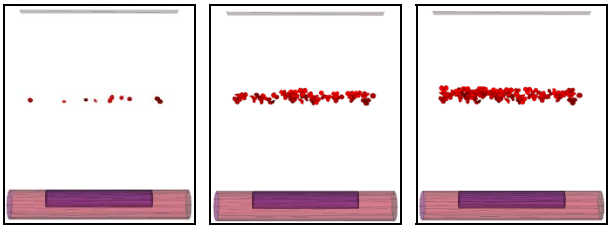

(b) 2.58 kN (79%F_p) (n_T=10, n_S=0)

(c) 3.14 kN (96%F_p) (n_T=107, n_S=0)

(d) 3.25 kN (99%F_p) (n_T=169, n_S=0)

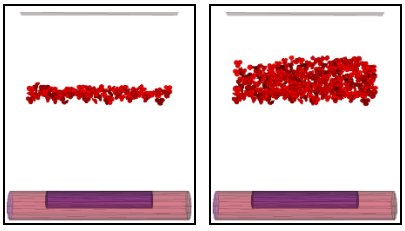

(e) 3.27 kN (100%F_p) (n_T=218, n_S=0)

(f) 2.16 kN (66%F_p) (n_T=770, n_S=0)

Fig. 9 Development of the failure process in the SCB numerical test of arrangement 4

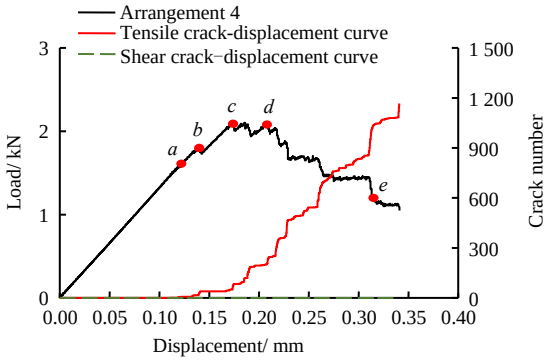

(a) Relationships between load, crack number and displacement

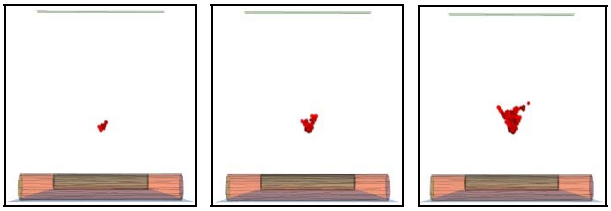

(b) 1.61 kN (77%F_p) (n_T=7, n_S=0)

(c) 1.80 kN (86%F_p) (n_T=28, n_S=0)

(d) 2.09 kN (100%F_p) (n_T=71, n_S=0)

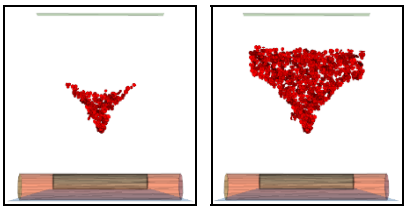

(e) 2.08 kN (99.5%F_p) (n_T=206, n_S=0)

(f) 1.20 kN (57%F_p) (n_T=1 039, n_S=0)

Fig. 10 Development of the failure process in the CCNSCB numerical test of arrangement 4

of a macro-crack. Afterwards, the cracks continue to grow steadily, and the load at point *c* reaches the maximum value of 3.11 kN. Then it enters the post-peak stage: the load drops approximately vertically from point *c* to point *e*, and the number of tension cracks increases sharply with extremely small displacements. Finally, a macro crack that penetrates the surface of the semi-disc is formed (see Fig.11). In addition, it is not difficult to find that the crack front is approximately linear during the entire progressive failure process.

The meso-scale numerical model I fracture toughness test of CCNSCB is divided into three stages: the initiation of the cracked chevron notch tip (point *a*), the stable growth of the cracked chevron notch (points *a*–*c*) and the penetrating stage (points *c*–*e*). The rupture process of the CCNSCB numerical test is similar to the indoor test. The load for the crack initiation is 1.61 kN, which is located at the tip of the chevron notch. The cracks are all tensile cracks, which is about 10% of the total number of cracks at the peak. Subsequently, the tensile cracks steadily propagate upward along the chevron notch, and the cracks are also tensile cracks. The load at load point *b* is 1.80 kN, which is about 86% of the peak load. Afterwards, it enters the stage of unsteady propagation and penetration: the load at point *c* reaches the maximum value of 2.09 kN. Meanwhile, the length of the mesoscopic tension crack reaches the critical value. Unlike the SCB specimen, the load in the CCNSCB test decreases stepwise from point *c* to point *e*. The tensile cracks extend from the chevron notch to the surface of the semi-circular disc, and then the number of cracks increases sharply with a small displacement, which is about 15 times the total number of cracks at the peak. At point *c*, the cracks increase sharply as the load decreases, and finally a macroscopic crack that penetrates the surface of the semi-disc is formed. During the whole process (from point *a* to *d*), the front edge of the crack is basically curved, which is different from the theoretically- assumed straight-through crack[18–19]. The discrete element model reflects the heterogeneity of the specimen.

The difference between CCNSCB and SCB tests is because different notch shapes correspond to different fracture mechanisms. The stress at the tip of the chevron notch is more concentrated than that of the straight notch, causing the bond at the tip to break first. When the crack extends to the root of the chevron notch, the length of the crack in space is the largest at this time and the stress is less concentrated than that at the tip of the chevron notch. The test requires a certain time step to intensify the stress concentration and cause the bond to break. Therefore, fluctuations can be observed in the load–displacement curve. The reason why the fracture toughness of CCNSCB specimens is generally higher than that of SCB specimens can also be explained from the perspective of numerical experiments.

Figures 11(a) and 11(b) show that there is a single macroscopic crack in the loading direction of the SCB and CCNSCB specimens in the laboratory test and the thin black line indicates the macroscopic crack. The fracture specimens of the numerical test are shown in Figs.11(c) and 11(d) and the red disc represents the meso-crack. These two cracks are comparable, and a macro-crack can be witnessed in the loading direction. Although the meso-cracks of the FJM3D model are discrete, a single macro-crack can still be clearly distinguished.

In addition, the macroscopic cracks of SCB and CCNSCB specimens in the laboratory test are generally parallel to the loading direction, and different degrees of distortion can be observed in the local cracks in Figs. 12(a) and 12(b) (local display range: $L_v = 10$ mm). Figures 12(c) and 12(d) show the stereonet projection of cracks at the end of the load, indicating that the cracks are mostly concentrated at the edge of the sphere. All cracks are parallel or nearly parallel to the loading direction, which is basically consistent with the results of the laboratory test.

(a) SCB failure specimen in the laboratory test

(b) CCNSCB failure specimen in the laboratory test

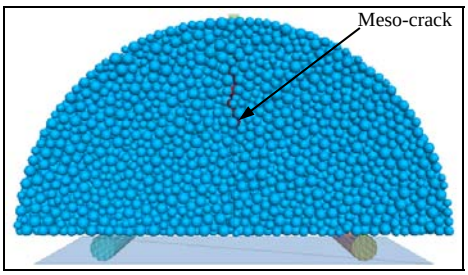

(c) SCB failure specimen in the numerical test

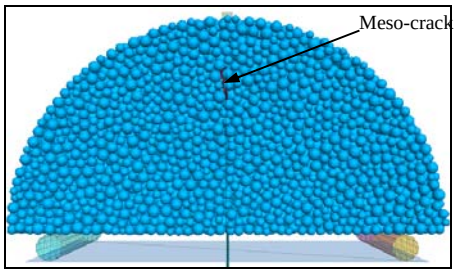

(d) CCNSCB failure specimen in the numerical test

Fig. 11 Failure specimens from laboratory tests[8] and a FJM3D simulation

4.3 Discussion on the tip stress state of mode I fracture toughness in numerical tests

In order to analyze the failure process of the SCB numerical specimens, seven measurement circles used to record the average horizontal stress are added between the straight-through notch of the FJM3D numerical specimen and the top load. To compare with the finite element results, the length of the straight notch of the SCB numerical model used in the calculation is 0.3*R*, the minimum particle diameter is 2.0 mm, the bond tensile strength is 20 MPa, and the other mesoscopic parameters are consistent with Table 1. Figure 13 shows the average horizontal stress–displacement curve and partially enlarged view of measurement circles 1–7. The horizontal stress of measurement circles 1 to 3 is tensile stress, and the horizontal stress of measurement circles 4 to 7 is compressive stress. Before the peak load, the horizontal stress increases with the increase of the load. When mesoscopic cracks appear at the tip of the straight notch, the stress of the measuring circle 1 drops suddenly, and it eventually approaches zero as the cracks increase. After the bond between particles in the measurement circle 1 is broken, the tip of the straight notch is extended correspondingly. The horizontal tensile stress in the measurement circle 2 increases instantly, and the bond breaks beyond the cut-off condition of bond tension. Similar phenomena are witnessed in the measurement circle 3. Before the peak load, the horizontal stress of measurement circles 4 and 5 basically does not change with the increase of the load. The tensile stress does not increase sharply until the mesoscopic crack penetrates to the vicinity of

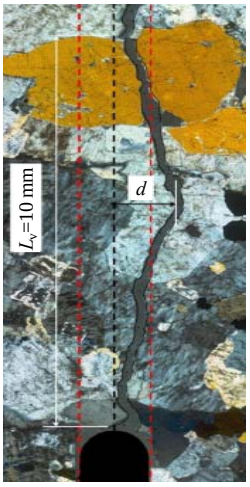

(a) SCB laboratory test

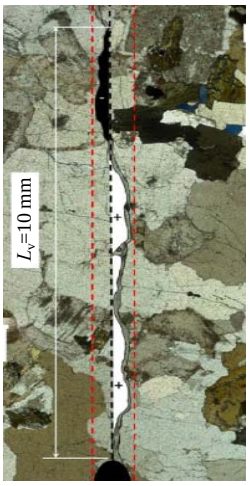

(b) CCNSCB laboratory test

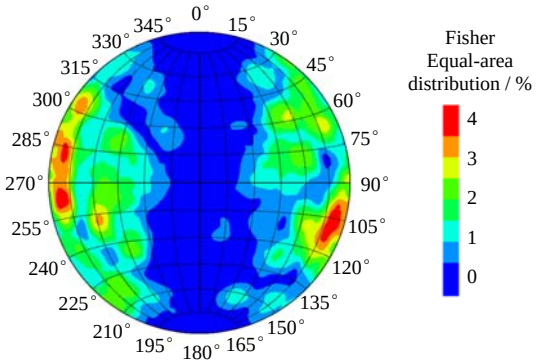

(c) SCB numerical test

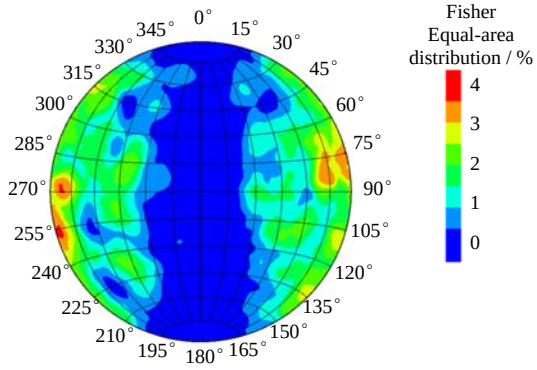

(d) CCNSCB numerical test

Fig. 12 Mesoscopic crack of laboratory tests and stereonet projections of cracks in the numerical test at 50% post-peak stress

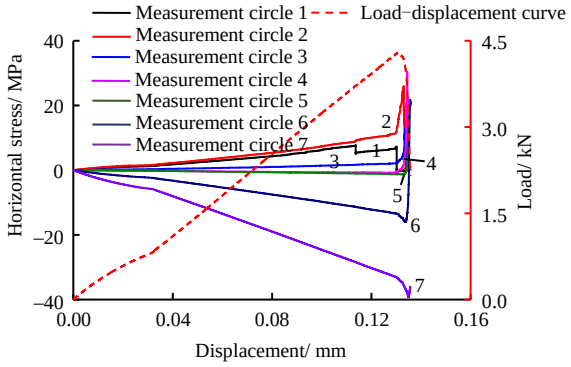

(a) Load, stress–displacement curves

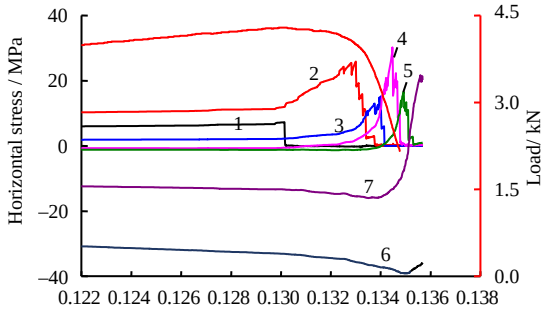

(b) Locally enlarged view

Fig. 13 Horizontal stress–displacement curve in the SCB test

these measurement circles after the peak. The horizontal compressive stress of measurement circles 6 and 7 is positively correlated with the load. When the crack penetrates to their attachment, the compressive stress is rapidly converted to tensile stress. The change and conversion of the stress at the tip well reflect the progressive failure process of the numerical SCB specimens. The horizontal stress distribution of each measurement circle at the peak load is compared with the calculated result of the continuous method[7] in Fig.14. Compared with the continuous method, the FJM3D numerical model provides a new perspective for the calculation of mode I fracture toughness. It has the following advantages: (1) some stresses of the measurement circles near the upper loading plate are converted from compressive stress to tensile stress; (2) the stress distribution and its discontinuous decrease can reflect the heterogeneity of the specimen.

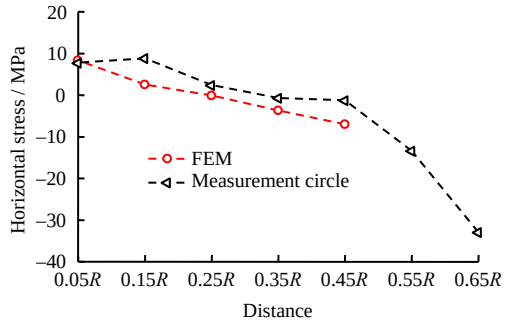

Fig. 14 Horizontal stress distributions from a FJM3D and continuum method in literature[7]

5 Conclusions

The flat joint model (FJM3D) is used in this study to systematically and deeply analyze the influencing factors of the mode I fracture toughness SCB tests and CCNSCB tests. By matching the SCB test and CCNSCB test of the Kowloon granite, its meso-fracture process can be investigated.

(1) A set of I-type fracture toughness test modeling method is developed. Multiple narrow bars are used, and the dividing wall is inserted to generate a semi-circular disc. The narrow wall is set up as the upper loading plate. Moreover, the straight-through notch and the cracked chevron notch are generated by DFN, which achieves smooth modeling and reduces the probability of model loading failure.

(2) The conclusions of the influencing factors of the model I fracture toughness test in FJM3D are as follows: the mode I fracture toughness K_{Ic} is positively correlated with the square root of average particle radius $\sqrt{R}$, average coordination number CN, and bond tensile strength σ_{b}, and negatively correlated with maximum/minimum particle diameter $d_{\max}/d_{\min}$ and S-type element fraction φ_{s}. There are no obvious linear relationships between K_{Ic} and model resolution Ψ, bond cohesion c_{b}, friction coefficient μ, friction angle φ. It is recommended that the model resolution should be kept above 11.8 and the maximum/ minimum particle diameter should be kept below 2 to obtain K_{Ic} with a small fluctuation.

(3) The FJM3D model is well matched with the SCB laboratory test results of the Kowloon granite. It is also verified that the mode I fracture toughness of the CCNSCB test can be matched by adjusting the maximum/minimum particle diameter $d_{\max}/d_{\min}$.

(4) By analyzing the crack propagation and horizontal stress distribution of the mode I fracture in SCB and CCNSCB tests, the failure mechanism of the semi-disc with different notch shapes is investigated. The crack initiation all happens at the tip of the notch, and the crack penetrates the upper loading plate along the loading radial direction. Additionally, the front edge of the crack in the SCB test is basically linear, while that in the CCNSCB test is basically curved. The conversion between the horizontal stress and the tensile stress of the semi-circular disc well reproduces the progressive failure mechanism of the semi-circular specimen in the three-point bending method.

References

[1] XU Ji-cheng, LIU Da-an, SUN Zong-qi, et al. International joint experiment study for the fracture toughness of rock materials[J]. Journal of Central South University of Technology, 1995, 26(3): 310–313.

[2] XU Xue-liang. Research on the experiment and meso-simulation of tensile characteristics and its fracture mechanism of brittle rock[D]. Beijing: University of Science and Technology Beijing, 2017.

[3] KURUPPU M D, OBARA Y, AYATOLLAHI M R, et al. ISRM-suggested method for determining the mode I static fracture toughness using semi-circular bend specimen[J]. Rock Mechanics Rock Engineering, 2014, 47(1): 267–274.

[4] ZHANG Sheng, WANG Long-fei, CHANG Xu, et al. Experimental study of size effect of fracture toughness of limestone using the notched semi-circular bend samples[J]. Rock and Soil Mechanics, 2019, 40(5): 1740–1749, 1760.

[5] DAI Feng, WEI Ming-dong, XU Nu-wen, et al. Progressive fracture mechanism of CCNSCB rock fracture toughness specimens and calibration of wide-range dimensionless stress intensity factors[J]. Rock and Soil Mechanics, 2016, 37(11): 3215–3223.

[6] WEI M D, DAI F, XU N W, et al. Experimental and numerical study on the cracked chevron notched semi-circular bend method for characterizing the mode I fracture toughness of rocks[J]. Rock Mechanics and Rock Engineering, 2016, 49(5):1595–1609

[7] WEI M D, DAI F, XU N W, et al. An experimental and theoretical assessment of semi-circular bend specimens with chevron and straight-through notches for mode I fracture toughness testing of rocks[J]. International Journal of Rock Mechanics and Mining Sciences, 2017, 99: 28–38.

[8] WONG L N Y, GUO T Y, WING K L. Experimental study of cracking characteristics of Kowloon granite based on three mode I fracture toughness methods[J]. Rock Mechanics and Rock Engineering, 2019, 52(11): 4217–4235.

[9] POTYONDY D O, CUNDALL P A. A bonded-particle model for rock[J]. International Journal of Rock Mechanics and Mining Sciences, 2004, 41(8): 1329–1364.

[10] YOON J. Application of experimental design and optimization to PFC model calibration in uniaxial compression simulation[J]. International Journal of Rock Mechanics and Mining Sciences, 2007, 44(6): 871–889.

[11] DING X B, ZHANG L Y. A new contact model to improve the simulated ratio of unconfined compressive strength to tensile strength in bonded particle models[J]. International Journal of Rock Mechanics and Mining Sciences, 2014, 69: 111–119.

[12] POTYONDY D O. PFC3D flat joint contact model version 1. Itasca Consulting Group[R]. Minneapolis: [s. n.], 2013.

[13] WU S C, XU X L. A study of three intrinsic problems of the classic discrete element method using flat-joint model[J]. Rock Mechanics and Rock Engineering, 2015, 49(5): 1813–1830.

[14] ITASCA. Particle flow code in 2 dimensions (version 3.1)[M]. Minneapolis: Itasca Cons Group, 2004.

[15] ZHANG X P, ZHANG Q. Distinction of crack nature in brittle rock-like materials: a numerical study based on moment tensors[J]. Rock Mechanics and Rock Engineering, 2017, 50, 2837–2845.

[16] TOMAC I, GUTIERREZ M. Coupled hydro-thermo-mechanical modeling of hydraulic fracturing in quasi-brittle rocks using BPM-DEM[J]. Journal of Rock Mechanics and Geotechnical Engineering, 2017, 9(1): 92–104.

[17] FENG P, AYATOLLAHI M R, DAI F, et al. DEM investigation on fracture mechanism of the CCNSCB specimen under intermediate dynamic loading[J]. Arabian Journal of Geosciences, 2017, 10(2): 48.

[18] WEI M D, DAI F, XU N W, et al. Experimental and numerical study on the cracked chevron notched semi-circular bend method for characterizing the mode I fracture toughness of rocks[J]. Rock Mechanics and Rock Engineering, 2016, 49(5): 1595–1609.

[19] OUCHTERLONY F. Suggested methods for determining the fracture toughness of rock[J]. International Journal of Rock Mechanics and Mining Sciences & Geo- mechanics Abstracts, 1988, 25(2): 71–96.